Localized adenosine signaling provides fine-tuned negative feedback over a wide dynamic range of neocortical network activities

Mark J. Wall and Magnus J. E. Richardson

J Neurophysiol 113:871-882, 2015. First published 12 November 2014; doi:10.1152/jn.00620.2014

J Neurophysiol 113: 871–882, 2015.
First published November 12, 2014; doi:10.1152/jn.00620.2014.

Localized adenosine signaling provides fine-tuned negative feedback over a wide dynamic range of neocortical network activities

Mark J. Wall[1] and Magnus J. E. Richardson[2]

[1]*School of Life Sciences, University of Warwick, Coventry, United Kingdom; and* [2]*Warwick Systems Biology Centre, University of Warwick, Coventry, United Kingdom*

Submitted 18 August 2014; accepted in final form 7 November 2014

Wall MJ, Richardson MJ. Localized adenosine signaling provides fine-tuned negative feedback over a wide dynamic range of neocortical network activities. *J Neurophysiol* 113: 871–882, 2015. First published November 12, 2014; doi:10.1152/jn.00620.2014.— Although the patterns of activity produced by neocortical networks are now better understood, how these states are activated, sustained, and terminated still remains unclear. Negative feedback by the endogenous neuromodulator adenosine may potentially play an important role, as it can be released by activity and there is dense A_1 receptor expression in the neocortex. Using electrophysiology, biosensors, and modeling, we have investigated the properties of adenosine signaling during physiological and pathological network activity in rat neocortical slices. Both low- and high-rate network activities were reduced by A_1 receptor activation and enhanced by block of A_1 receptors, consistent with activity-dependent adenosine release. Since the A_1 receptors were neither saturated nor completely unoccupied during either low- or high-rate activity, adenosine signaling provides a negative-feedback mechanism with a wide dynamic range. Modeling and biosensor experiments show that during high-rate activity increases in extracellular adenosine concentration are highly localized and are uncorrelated over short distances that are certainly < 500 μm. Modeling also predicts that the slow rise of the purine waveform cannot be from diffusion from distal release sites but more likely results from uptake and metabolism. The inability to directly measure adenosine release during low-rate activity, although it is present, is probably a consequence of small localized increases in adenosine concentration that are rapidly diminished by diffusion and active removal mechanisms. Saturation of such removal mechanisms when higher concentrations of adenosine are released results in the accumulation of inosine, explaining the strong purine signal during high-rate activity.

adenosine; biosensor; diffusion; modulation; neocortex

THE NEOCORTEX SUPPORTS a range of different network activities that underlie its importance in cognitive function. These range from slow wave oscillations (Steriade et al. 1993) to sustained bursts of high-frequency activity that occur in pathological states such as epilepsy (Grenier et al. 2003). Acute in vitro slice preparations have been developed that, through manipulation of artificial cerebrospinal fluid (aCSF) composition, provide powerful experimental tools for analyzing the roles that synaptic and cellular components play in supporting these states (for example, see Sanchez-Vives and McCormick 2000; Silberberg et al. 2004). However, the precise nature of these states is still unclear (Frohlich and McCormick 2010; Parga and Abbot 2007), and in particular there remains intense debate as to the generative mechanism of their dynamics. One candidate mechanism is negative feedback provided by the activity-dependent release of an endogenous neuromodulator such as adenosine.

The purine adenosine is a potent neuromodulator, central to many CNS processes, including sleep, memory formation, and locomotion, and can be neuroprotective (depending on brain region and stage of development) during epilepsy, hypoxia, and ischemia (reviewed in Boison 2009; Dale and Frenguelli 2009; Fredholm 1996). Adenosine activates cell surface G protein-coupled receptors, with the widely distributed high-affinity A_1 receptor inhibiting transmitter release and hyperpolarizing the membrane potential (reviewed in Fredholm et al. 2000). Once released, adenosine is rapidly removed by uptake and is subsequently converted either to AMP by adenosine kinase (ADK; primarily in glial cells) or to inosine and hypoxanthine by adenosine deaminase (ADA) and purine nucleoside phosphorylase (PNP) (reviewed in Dunwiddie and Masino 2001). Trains of action potentials increase the concentration of extracellular adenosine (activity-dependent adenosine release) in many brain regions including the hippocampus (Lovatt et al. 2012; Mitchell et al. 1993; Wall and Dale 2013), calyx of Held (Kimura et al. 2003; Wong et al. 2006), supraoptic nucleus (Oliet and Poulain 1999), striatum (Pajski and Venton 2010), and cerebellum (Wall and Dale 2007). It has been known for many years that adenosine release occurs during high-rate pathological activity, such as epileptic seizures, where it acts to reduce the frequency and duration of subsequent seizures (Boison 2008; Dale and Frenguelli 2009; During and Spencer 1992). Recent studies have shown that only a small number of action potentials at physiological frequencies are required to increase the extracellular adenosine concentration sufficiently to inhibit synaptic transmission (Lovatt et al. 2012; Wall and Dale 2013). Thus, during low-rate activity states, the release of adenosine and activation of A_1 receptors could control the degree of network activation, terminate events, and prevent physiological activity from becoming pathological.

We hypothesize that adenosine plays an important role in controlling neocortical network activity because A_1 adenosine receptors are strongly expressed by thick-tufted layer V pyramidal cells (Ochiishi et al. 1999; Rivkees et al. 1995), where they potently inhibit synaptic transmission (Kerr et al. 2013) and hyperpolarize the membrane potential (van Aerde et al. 2013). In this study we have investigated the role of adenosine in physiological and pathological neocortical network activity induced by either excitant solution (as a model of the up-down states observed in vivo) or Mg^{2+}-free aCSF (as a model of higher-rate pathological, epileptic-like activity). Our results demonstrate that adenosine provides highly localized negative-

Address for reprint requests and other correspondence: M. J. Wall, School of Life Sciences, Univ. of Warwick, Gibbet Hill, Coventry, CV4 7AL, UK (e-mail: mark.wall@warwick.ac.uk).

feedback control that is effective over a wide range of activity intensities.

MATERIALS AND METHODS

Preparation of neocortical slices. Experiments were approved by the Animal Welfare and Ethical Review Body (AWERB). Sagittal slices of hindlimb somatosensory neocortex (350–400 μm) were prepared from male Wistar rats at postnatal days 18–25 (Kerr et al. 2013). Rats were kept on a 12:12-h light-dark cycle with slices made 90 min after entering the light cycle. In accordance with the UK Animals (Scientific Procedures) Act (1986), male rats were killed by cervical dislocation and decapitated. The brain was removed and cut down the midline and the two sides of the brain stuck down. Slices were cut around the midline with a Microm HM 650V microslicer in cold (2–4°C) high-Mg^{2+}, low-Ca^{2+} aCSF, composed of (mM) 127 NaCl, 1.9 KCl, 8 $MgCl_2$, 0.5 $CaCl_2$, 1.2 KH_2PO_4, 26 $NaHCO_3$, and 10 D-glucose (pH 7.4 when bubbled with 95% O_2-5% CO_2, 300 mosM). Slices were trimmed so that only the neocortex was present and stored at 34°C for 30 min in aCSF (1 mM $MgCl_2$, 2 mM $CaCl_2$) and then at room temperature for 1–6 h.

Patch-clamp recording from layer V neurons. A slice (350 μm) was transferred to the recording chamber and perfused at 3 ml/min with aCSF at 32 ± 0.5°C. Slices were visualized with IR-DIC optics with an Olympus BX51W1 microscope and a Hitachi CCD camera (Scientifica, Bedford, UK). Whole cell current-clamp recordings were made from layer V pyramidal cells with patch pipettes (5–10 MΩ) manufactured from thick-walled glass (Harvard Apparatus, Edenbridge, UK) and containing (mM) 135 potassium gluconate, 7 NaCl, 10 HEPES, 0.5 EGTA, 10 phosphocreatine, 2 MgATP, and 0.3 NaGTP, with 1 mg/ml biocytin (290 mosM, pH 7.2). Layer V pyramidal cells were identified by their position in the slice, current-voltage relationship, and morphology. Voltage recordings were obtained with an Axon Multiclamp 700B amplifier (Molecular Devices) and digitized at 20 kHz. Data acquisition and analysis were performed with pCLAMP 9 (Molecular Devices). In some experiments whole cell patch-clamp recording was combined with either extracellular recording or biosensor measurements (see below).

Extracellular and biosensor recording from neocortical slices. A slice (400 μm) was transferred to the recording chamber, submerged in aCSF, and perfused at 6 ml/min (32°C). The slice was placed on a grid allowing perfusion above and below the tissue, and all tubing was gastight (to prevent hypoxia). For extracellular recording, two aCSF-filled microelectrodes were placed on the surface of layer V (1–3 mm apart). Extracellular recordings were made with ISO-DAM amplifiers (WPI, Stevenage, UK). Signals were filtered at 3 kHz and digitized online (10 kHz) with a Micro CED (Mark 2) interface controlled by Spike software (version 6.1, Cambridge Electronic Design, Cambridge, UK). Standard cylindrical microelectrode biosensors were inserted into the slice so that biosensors went through the slice, and disk biosensors were gently pushed into the slice surface.

Biosensor characteristics. Biosensors (Sarissa Biomedical, Coventry, UK) consisted of enzymes trapped within a matrix around a Pt or Pt/Ir (90/10) wire (Llaudet et al. 2003). Biosensors were of two types: cylinders that had an exposed length of ~500 μm and diameter of ~50 μm and disk sensors that had a diameter of 125 μm. Four types of sensor were used in this study: first, null sensors, possessing the matrix but no enzymes, to control for nonspecific electro-active interferents; second, biosensors containing ADA, nucleoside phosphorylase, and xanthine oxidase (responsive to adenosine, inosine, and hypoxanthine: ADO biosensors); third, biosensors containing nucleoside phosphorylase and xanthine oxidase (responsive to inosine and hypoxanthine: INO biosensors); and finally, biosensors containing xanthine oxidase (responsive to hypoxanthine: HYP biosensors).

A full description of biosensor properties has previously been published (Llaudet et al. 2003). After each experiment, the biosensors were calibrated with analyte (10 μM). In some experiments, the composition of purines detected by ADO biosensors was not fully defined. Since ADO biosensors have an equal sensitivity to adenosine, inosine, and hypoxanthine (Llaudet et al. 2003; Wall et al. 2007), the total concentration of purines detected was related to the calibration to adenosine to give μM′ or nM′ of purines (as outlined in Klyuch et al. 2011; Pearson et al. 2001). Biosensor signals were acquired at 1 kHz with a Micro CED (Mark 2) interface using Spike (version 6.1) software.

Purine diffusion model. We construct a basic mathematical model that can be used to provide an upper bound on the distance that adenosine travels once released into the extracellular space. To this end, we neglect removal by cellular uptake and combine together the adenosine, inosine, and hypoxanthine concentrations into a single purine concentration $C(t)$, which obeys diffusive dynamics

$$\frac{\partial C}{\partial t} = D\nabla^2 C \tag{1}$$

where D is the diffusion constant. Two scenarios are considered: *1*) the in vitro slice preparation, of thickness h, with a zero-concentration condition at the top and bottom slice surfaces and *2*) free diffusion, which is more similar to the in vivo case. For the first case we consider that the variable z measures the distance normal to the surfaces of the slice at $z = h/2$ and $-h/2$ and r measures a distance parallel to the slice surface. The Fourier-series solution for an initial sheetlike concentration, uniform in x and y at the center of the slice (Klyuch et al. 2011), can be adapted to the case of an initial pointlike source at position $x = y = z = 0$, by simply multiplying that result with a two-dimensional Gaussian that is a function of the variable $r^2 = x^2 + y^2$. The resulting space- and time-dependent concentration can be written as

$$C = \frac{\exp(-r^2/4Dt)}{4\pi Dt}\frac{2}{h}\sum_{m=0}^{\infty}\exp(-t/\tau_m)\cos\left(\frac{(2m+1)\pi z}{h}\right) \tag{2}$$

where the time constants τ_m are defined as

$$\tau_m = \frac{h^2}{(2m+1)^2\pi^2 D}. \tag{3}$$

Equation 2 gives the concentration for an initial short release event of unit amplitude at time $t = 0$ within the slice at the origin. Setting $z = 0$ in the above equation gives the concentration at a distance r from the release site in the center of the slice. The time constant, $\tau_0 = h^2/\pi^2 D$, of the longest decay can be used to estimate the effective diffusion constant in tissue. The solution given by *Eq. 2* can also be written in terms of Gaussians using the method of images. This is a method used in the physics of charged particles that makes use of the linearity of the problem. It accounts for the zero-concentration boundaries through the addition to the point source at $x = y = z = 0$ of fictitious sources at distances $z = h$, $2h$, $3h$, etc. from the center. These have freely diffusing concentrations (3-dimensional Gaussian solution) that have alternating signs. However, the first term of such a series solution is simply identical to the diffusion in the in vivo geometry (with no slice surfaces) where here $r^2 = x^2 + y^2 + z^2$

$$C = \frac{\exp(-r^2/4Dt)}{(4\pi Dt)^{3/2}}. \tag{4}$$

This equation behaves closely to that for the slice geometry (*Eq. 2*) at times $< h^2/4D$, which are before any purine molecules are likely to have reached the slice surface. In plotting the purine concentrations $C(t)$, the waveforms were filtered with an additional exponential filter of time constant 1 s to mimic the rise time constant on the purine biosensors.

Deconvolution and reconvolution of purine waveforms. The amplitude of closely spaced purine waveforms can be difficult to measure, as subsequent pulses sit on the decay of proceeding ones. Following

Richardson and Silberberg (2008), closely spaced purine pulses were deconvolved as in Klyuch et al. (2011) by removing the long decay τ_0 component. The resulting sharper, well-spaced pulses could then be cropped and reconvolved to yield isolated purine waveforms from which the amplitude could be directly measured.

Drugs. All drugs were made up as 10–100 mM stock solutions, stored frozen, and then thawed and diluted with aCSF on the day of use. Adenosine, inosine, hypoxanthine, and 8-cyclopentyltheophylline (8-CPT) were purchased from Sigma (Poole, UK). *Erythro*-9-(2-hydroxy-3-nonyl)adenine (EHNA) was purchased from Tocris-Cookson (Bristol, UK).

Data analysis. Data are presented as means ± SE. Statistical analysis was performed with Student's *t*-test. The significance level was set at $P < 0.05$.

Induction of cortical network activity. In control conditions, neocortical slices are essentially quiescent, with spontaneous network activity extremely infrequent. Thus, in common with previous studies, network activity was induced by altering the ionic composition of the extracellular solution (aCSF). Two different extracellular solutions were used to excite network activity: excitant solution to induce up-down state-like activity (aCSF with 0.5 mM Mg^{2+}, 6.5 mM K^+, 1.5 mM Ca^{2+}; Sanchez-Vives and McCormick 2000; Silberberg et al. 2004) and zero-Mg^{2+} aCSF (0 mM Mg^{2+}, 3.5 mM K^+, 2 mM Ca^{2+}) to induce strong epileptiform-like activity (Gulyás-Kovács et al. 2002; Mody et al. 1987; Traub et al. 1994). It took 10–15 min for network activity to commence, and there was a progression in the level of excitation until steady-state conditions occurred, reflecting the slow time to alter ionic concentrations deep within the slices. Network activity was defined as coordinated activity on two electrodes, which includes extracellular electrodes, biosensors (as they also act as extracellular electrodes; Dale et al. 2000), and intracellular recordings from pyramidal cells.

RESULTS

Adenosine A_1 receptors modulate low-rate neocortical network activity. Perfusion of slices with excitant solution induced coordinated network activity, defined as correlated activity on both extracellular electrodes (Fig. 1*A*). In 16 of 18 slices (88%) activity consisted of single and small groups (2–5) of population spikes (Fig. 1*A*), with a population spike defined as an isolated change in potential (Fig. 1*A*, *inset*). In two slices, longer bursts of activity were also observed. The frequency of activity was 0.1 ± 0.02 Hz ($n = 18$), which is approximately six events per minute. Whole cell patch-clamp recordings from layer V pyramidal cells revealed that a single extracellular population spike was equivalent to a short-lived membrane depolarization (~200–300 ms) with one to five superimposed action potentials (frequency 10–25 Hz; Fig. 1*B*, $n = 5$). Groups of these depolarized states could occur together, on occasion, with a high-frequency component, similar to that induced by zero-Mg^{2+} aCSF (see below).

To investigate whether the network activity induced by excitant solution can be modulated by adenosine receptor activation, adenosine (100 μM) was applied. Adenosine either abolished or greatly reduced the frequency of coordinated activity (activity abolished in 6 slices, frequency reduced from 0.1 to 0.001 Hz in 2 slices). Infrequent activity could sometimes be observed on individual electrodes, but this was no longer coordinated across the network (Fig. 1*A*). The effects of adenosine could be reversed in wash or by application of the A_1 receptor antagonist 8-CPT (2 μM, $n = 5$).

To investigate whether A_1 receptors are activated and functional during network activity, the A_1 receptor antagonist

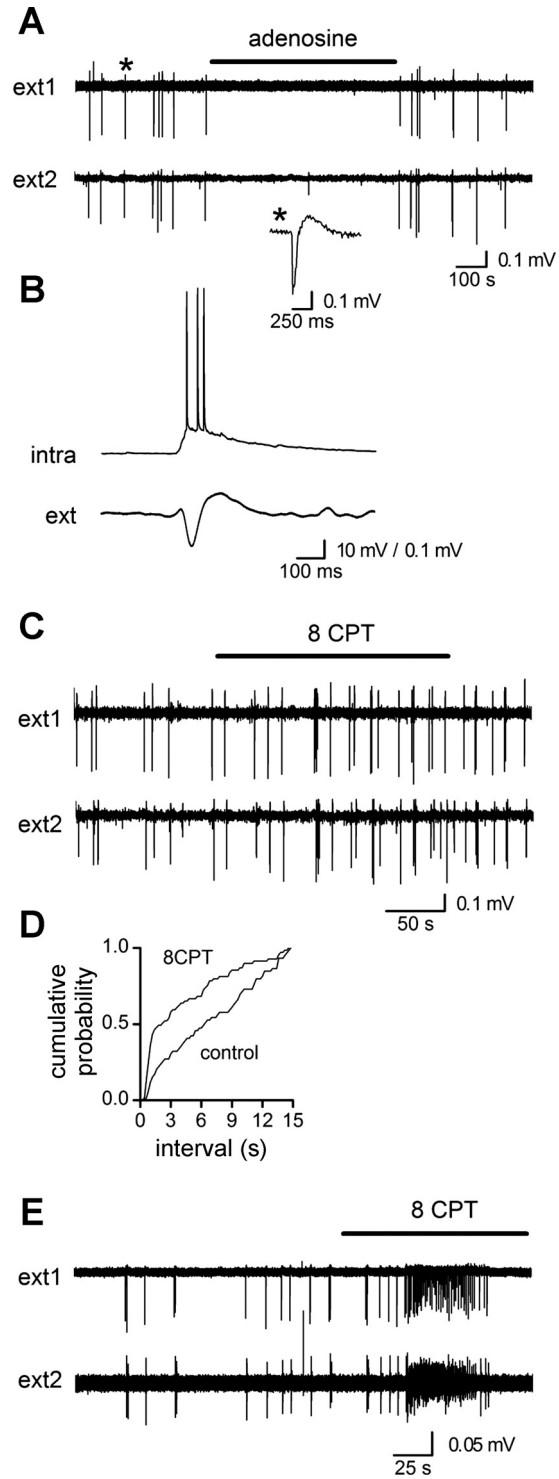

Fig. 1. Low-rate neocortical network activity is modulated by adenosine. *A*: coordinated network activity measured on 2 extracellular electrodes (*ext1*, *ext2*). Adenosine (100 μM) abolished network activity, which recovered in wash. *Inset*, a single extracellular population spike (*), at an expanded time base. *B*: whole cell patch-clamp recording from a layer V pyramidal cell (intra) with simultaneous extracellular recording of a population spike (ext). *C*: coordinated network activity on 2 extracellular electrodes. The A_1 receptor antagonist 8-cyclopentyltheophylline (8-CPT, 1 μM) increased burst duration and frequency. *D*: plot of cumulative probability for event intervals derived from the data in *C*. *E*: coordinated network activity measured on 2 extracellular electrodes. The A_1 receptor antagonist 8-CPT (1 μM) induced a prolonged burst of activity. In all experiments, network activity was induced by incubation in excitant solution.

8-CPT was applied. Blocking A_1 receptors significantly ($P < 0.01$) increased the frequency of network events (from 0.084 ± 0.03 to 0.145 ± 0.05 Hz; a reduction in interevent interval from ~12 to 7 s, $n = 9$ slices; Fig. 1*C*). Examination of interevent intervals revealed an increase in the probability of an event occurring within the first few seconds of the previous event, suggesting that the activation of A_1 receptors plays a role in terminating and subsequently suppressing activity (Fig. 1*D*). In some slices ($n = 4$) blockade of A_1 receptors with 8-CPT also induced bursts of sustained activity, which were similar to that observed in zero-Mg^{2+} aCSF (Fig. 1*E*; mean duration 88 ± 33 s, see below), suggesting that activation of A_1 receptors can prevent transition from physiological to pathological states. The increase in network excitability following block of A_1 receptors is consistent with adenosine being released into the extracellular space by activity.

Actions of adenosine during high-rate pathological network activation. To induce high-rate network activity, slices were perfused with aCSF that did not contain magnesium (zero-Mg^{2+} aCSF). This solution reliably induced spontaneous activity (13 of 13 slices) with activity patterns that ranged from frequent population spikes to sustained bursts of activity (mean burst length 32 ± 3 s, burst frequency 0.02 ± 0.01 Hz, ~1 burst/min; Fig. 2*A*). Whole cell patch-clamp recordings from layer V pyramidal cells revealed that each burst consisted of an initial period of continuous action potential firing (10–100 Hz) followed by individual bursts made up of one to five action potentials (fired at 10–25 Hz) superimposed on short depolarizations (Fig. 2*B*; $n = 5$).

To confirm that neocortical network activity induced by zero-Mg^{2+} aCSF could be modulated by adenosine receptor activation (see O'Shaughnessy et al. 1988), adenosine (100 μM) was applied. In seven of seven slices, application of adenosine greatly reduced network activity (Fig. 2*A*). The frequency of bursts was reduced from 0.017 ± 0.01 Hz to 0.005 ± 0.0023 Hz, less than one burst every 3 min. Burst duration was decreased from 30.5 ± 4.44 to 8.2 ± 5 s, with, in some slices, bursts converted to isolated population spikes. The effects of adenosine could be reversed in wash or by application of the A_1 receptor antagonist 8-CPT (1–2 μM, Fig. 2*A*; $n = 4$).

To investigate whether there is activation of A_1 receptors during the network activity induced by zero-Mg^{2+} aCSF, the A_1 receptor antagonist 8-CPT was applied. In eight of eight slices, 8-CPT (1–2 μM) caused an increase in network excitation, a fall in the time interval between bursts, and an increase in the frequency of events within a burst (with events considered separate if they occurred >0.5 s apart; Fig. 2*C*). The interval between bursts was reduced from to 16.5 ± 0.8 s to 4.6 ± 1.7 s, with the frequency of events within a burst increasing from 0.34 ± 0.2 Hz to 0.83 ± 0.3 Hz. In some slices, discrete bursts of activity became almost continuous, with no obvious quiescent periods between bursts. This suggests that endogenous activation of A_1 receptors plays a role in the termination of activity preventing continual network activation. Thus, as with many former studies (particularly in the hippocampus), pathological network activity is enhanced by blocking A_1 receptors and the quiet periods between bursts are at least in part caused by the actions of adenosine.

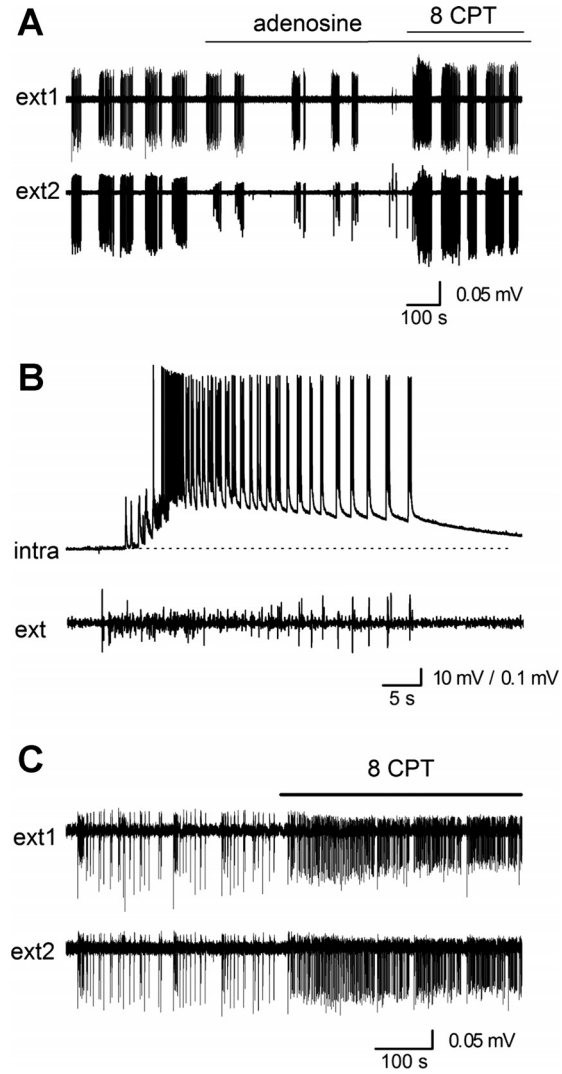

Fig. 2. Adenosine modulates pathological high-rate network activity. *A*: coordinated activity on 2 extracellular electrodes. Adenosine (100 μM) reduced the frequency of burst occurrence, burst duration, and spike amplitude. Addition of the A_1 receptor antagonist 8-CPT (1 μM) reversed the effects of adenosine. *B*: whole cell-patch clamp recording from a layer V pyramidal cell with simultaneous extracellular recording during a burst of activity. *C*: coordinated activity on 2 extracellular electrodes. Application of 8-CPT (1 μM) greatly increased activity, with no pauses between bursts. Network activity was induced by incubation in zero-Mg^{2+} aCSF. The marked differences in activity illustrated in *A* and *C* reflect variations across slices.

Measuring adenosine release directly with biosensors during low-rate activity. Low-rate network activity induced by excitant solution was enhanced by blocking A_1 receptors, which is consistent with an increase in the concentration of extracellular adenosine during activity. To investigate this, ADO biosensors and null sensors were placed within layer V to directly measure changes in extracellular adenosine concentration during activity. Although excitant solution always induced activity, in the majority of slices (11 of 14) this did not increase the ADO biosensor current compared with the null sensor (Fig. 3, *A* and *B*). There was also no clear increase in ADO biosensor current immediately following a single population spike or a group of population spikes (Fig. 3, *A* and *B*). The fast deflections present on the ADO biosensor occur at the same time as the extracellular electrode (and null sensor) and have the same

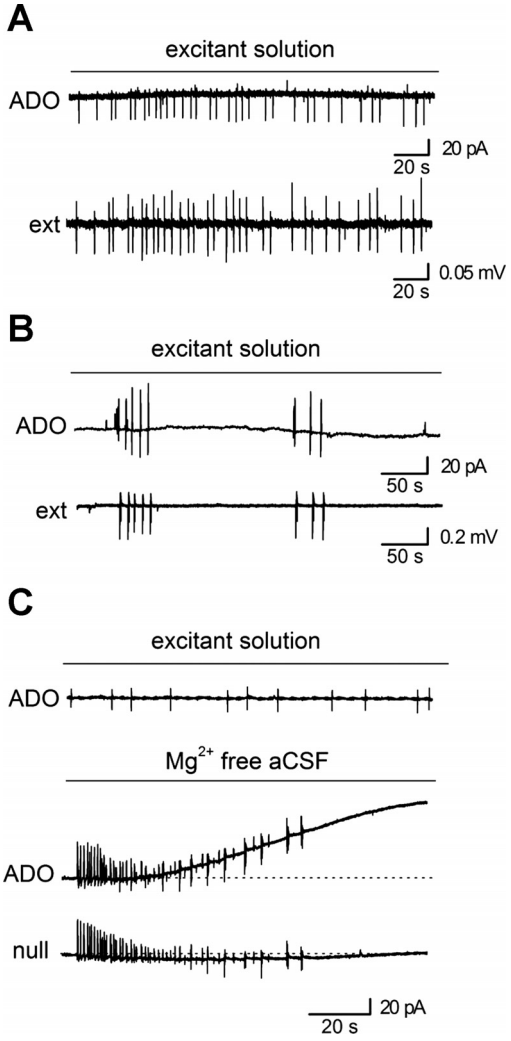

Fig. 3. Biosensors do not reliably detect an increase in extracellular purine concentration with activity induced by excitant solution. *A*: coordinated activity on an adenosine biosensor (ADO) and an extracellular electrode (ext) induced by excitant solution. There was no change in the amplitude of the biosensor baseline current during activity (same as null trace, which is not illustrated). The fast deflections on the ADO biosensor trace are due to detection of electrical activity, not changes in purine concentration. *B*: coordinated activity, consisting of groups of population spikes, recorded on an adenosine biosensor and an extracellular electrode. There was no increase in biosensor current following each group of population spikes. *C*: when activity was induced with excitant solution there was no detectable increase in extracellular purine concentration measured by the ADO biosensor (*top*). However, when Mg^{2+}-free aCSF was applied to the same slice, a robust current was measured on the ADO biosensor, with no increase in current on the null sensor (*bottom*).

duration, and thus are produced by electrical activity [action potentials and excitatory postsynaptic potentials (EPSPs)] rather than purine detection. Although the detection of electrical events by the biosensor shows that the network is active around the biosensor, there was no detectable increase in the concentration of extracellular adenosine (or metabolites) during activity. Thus if adenosine is being released, the concentration may be lower than the limits of detection (~25 nM, see below) or there may be local release and the adenosine is rapidly removed from the extracellular space.

To confirm the validity of our results we carried out a number of controls. First, to confirm that the damage produced by biosensor insertion did not prevent adenosine detection, biosensors were placed parallel to the slice surface (Klyuch et al. 2011; Wall and Dale 2013). This did not reveal a current on the ADO biosensor during excitant-induced activity ($n = 5$, data not shown). To confirm that an increase in extracellular adenosine concentration (or metabolite concentration, as the biosensor also detects adenosine metabolites, see below) could be detected, either the Mg^{2+} concentration of excitant solution was lowered (to between 0.3 and 0 mM) or A_1 receptors were blocked with 8-CPT. This reliably produced large biosensor currents (Fig. 3*C*), but these were associated with bursts of activity rather than single or groups of population spikes. To check whether the extracellular concentration of adenosine (or its metabolites) is increased in other cortical layers, ADO biosensors were placed into layer 2/3. This did not reveal biosensor currents during excitant-induced activity, although zero-Mg^{2+} aCSF induced large ADO biosensor currents (5 of 5 slices) similarly to what was seen in layer 5 (data not shown).

Adenosine release can be directly measured during high-rate activity. In most slices, the activity induced by excitant solution (single or small groups of population spikes) did not lead to a directly detectable increase in extracellular adenosine (or metabolite) concentration. However, in a small minority of slices (3 of 14) small but unambiguous increases in ADO biosensor current were observed, which were absent on the null sensor (Fig. 4*A*). When examined carefully, it was found that the activity consisted of population spikes followed by high-frequency activity (Fig. 4*A*, *inset*). For further investigation, we combined whole cell patch-clamp recordings with low-rate excitant solution, with the Mg^{2+} varied from 0.5 to 0.3 mM to induce different strengths of activity. When pyramidal cell activity was equivalent to single population spikes (0.5 mM Mg^{2}) there was no detectable increase in extracellular purine concentration ($n = 7$; Fig. 4*B*). However, when Mg^{2+} was lowered (to 0.3 mM) clear biosensor signals could be observed ($n = 4$; Fig. 4, *C* and *D*). In most of the pyramidal cell recordings activity appeared prolonged and the depolarization larger than with 0.5 mM Mg^{2+}, indicative of greater network activity (Fig. 4, *C* and *D*). Thus although the form of activity required to produce detectable concentrations of adenosine is not radically different from when adenosine cannot be measured, greater network activity is required. In Fig. 4*C*, although a large biosensor current was produced by the initial activity, subsequent activity was not detected on the biosensor and there was no change in the gradient of the biosensor current. This suggests that adenosine (or metabolites) may only be detected locally, where the network is active.

Properties of adenosine release induced by zero-Mg^{2+} aCSF. We used the data from pathological high-rate network activity combined with simulations to analyze the properties of adenosine release, diffusion, and metabolism. In zero-Mg^{2+} aCSF, each burst of neural activity induced a current on the ADO biosensor, with no effect on the null sensor baseline current (Fig. 5*A*; $n = 6$). Deconvolution-reconvolution analysis (see MATERIALS AND METHODS) of the overlapping events on the ADO biosensor allowed for separation into component waveforms, facilitating measurement of amplitude and kinetics (Fig. 5*B*). The mean amplitude of the current produced by the first burst of neural activity was 422 ± 200 pA, which is equivalent to 3.4 ± 1.1 $\mu M'$ of purines (range 0.1–13 $\mu M'$, $n = 14$). The

large variability in the amount of purines detected presumably stems from differences in the amount of neural activity (number of cells activated and duration of the activity) and distance from release sites.

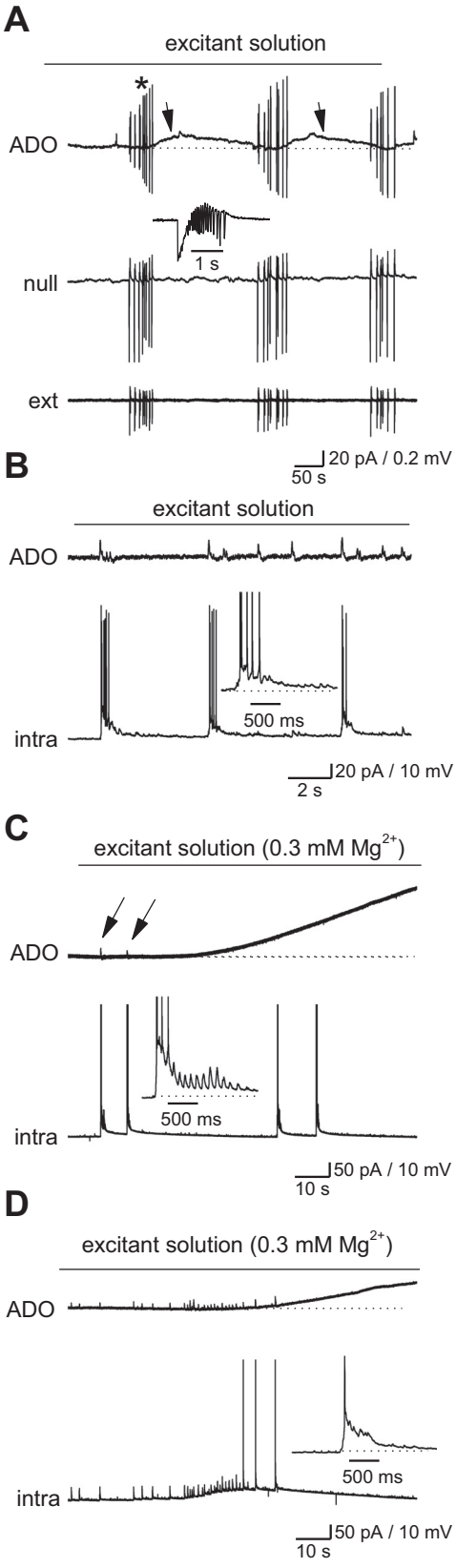

Since ADO biosensors respond not only to adenosine but also to inosine and hypoxanthine (adenosine metabolites; Llaudet et al. 2003) with approximately equal sensitivity, the ADO biosensor signal could be produced by adenosine alone, adenosine metabolites, or a combination of both. Thus the ADA inhibitor EHNA (Agarwal et al. 1977) was used to determine the proportion of the purines detected that arise from the extracellular metabolism of adenosine (Klyuch et al. 2011; Wall and Dale 2007, 2013). EHNA prevents the conversion of adenosine to inosine (by ADA) in the slice and also prevents ADO biosensors detecting adenosine, with no effect on the detection of inosine or hypoxanthine (Wall and Dale 2007). If adenosine is directly detected or any inosine (or hypoxanthine) detected arises from the metabolism of adenosine by ADA, then EHNA will reduce the amplitude of the biosensor signal (Klyuch et al. 2011; Wall and Dale 2007, 2013). Conversely, if the biosensor signals arise from the direct release of inosine or hypoxanthine into the extracellular space, then EHNA will have no effect on the signal amplitude (Wall et al. 2010). After the induction of network activity (with zero-Mg^{2+} aCSF) and resultant purine release, EHNA (20 μM) was applied (2 μM of A_1 receptor antagonist 8-CPT was also present to prevent accumulation of adenosine reducing neural activity). EHNA reduced the ADO biosensor signal by 74 $\pm$ 5% (Fig. 5*C*; n = 5), and thus either adenosine is directly detected or the biosensor signal arises from the metabolism of adenosine by ADA in the slice.

The ADO biosensor waveform had a slow time to rise of 108 $\pm$ 10 s (n = 10; Fig. 5*D*). This slow rise was not determined by the response time of the biosensor, as it is much slower than biosensor calibration traces (rise typically ~10–15 s; Fig. 5*D*), which are limited by the rate of bath exchange rather than speed of biosensor response. For fast applications of adenosine the biosensor response time is of the order of 1 s (Fig. 5*D*, *bottom*). We also observed that the signal on the ADO biosensor is delayed and did not start to rise until around the middle of bursts of activity (Fig. 5*E*; also see Fig. 4*C*). The delay and slow rise suggest that either adenosine or its metabolites have to diffuse to the biosensor from distant release sites or sufficient adenosine has to be released to saturate efficient removal

Fig. 4. Network activity required for the biosensor detection of adenosine or metabolites. *A*: coordinated activity (induced by excitant solution) recorded on an adenosine biosensor, null sensor, and an extracellular electrode (ext). There was an increase in ADO biosensor current following each group of population spikes. *Inset*, a single event from *A* (ext at asterisk) consists of a population spike followed by a train of high-frequency activity. *B*: coordinated activity (induced by excitant solution) recorded on an adenosine biosensor and an intracellular recording from layer V pyramidal cell (intra). Short-lived depolarized states (equivalent to population spikes) did not produce an increase in ADO biosensor current. *Inset*, a single burst of intracellular activity at an expanded time base. *C*: coordinated activity recorded on an adenosine biosensor and an intracellular recording from layer V pyramidal cell. In this recording there was a clear increase in the ADO biosensor current following initial network activity (arrows). *Inset*, a single burst of intracellular activity at an expanded time base. Although more action potentials are fired in *B*, activity in *C* is prolonged with greater depolarization and more excitatory postsynaptic potentials (EPSPs) and thus represents greater network activation. *D*: coordinated activity recorded on an adenosine biosensor and an intracellular recording from a layer V pyramidal cell. In this recording there was a clear increase in the ADO biosensor current following activity, which consists of a number of EPSPs indicating network activation. *Inset*, a single burst of intracellular activity at an expanded time base. The spikes in the *insets* have been truncated.

mechanisms and reach the biosensor, directly or in the form of metabolites. The decay of the ADO biosensor waveform was also slow (decay time constant of ~200 s, $n = 5$; see Fig. 5, *A* and *B*, and compare with Fig. 5*D*, *bottom*), which is consistent with the slow loss of purines from the slice surface into the bath medium (Klyuch et al. 2011).

The slow purine waveform is not the result of diffusion. We used mathematical models and simulations to investigate whether it is feasible for the slow (100 s) rise of the ADO biosensor signal to result from the diffusion of adenosine or its metabolites from distal release sites. The role of this model is not to capture adenosine transport in detail but to provide an upper bound on the distance adenosine will travel by ignoring removal mechanisms. We examined two models: a model that accounts for the in vitro configuration (*Eq. 2*) of the slice (with top and bottom surfaces open to the bathing medium) and a model that has free diffusion (*Eq. 4*) and is therefore similar to the in vivo geometry. Following Klyuch et al. (2011), we used the 200-s decay time constant of the waveform to provide a model-dependent estimate of the effective diffusion constant of adenosine in the neocortex as 80 $\mu m^2/s$, which is lower than that estimated for the cerebellum (~250 $\mu m^2/s$) and also than that expected on the grounds of tortuous diffusion in the extracellular space, potentially reflecting the action of distinct transport mechanisms in the neocortex. Model plots (Fig. 6*A*) of the purine concentration waveform at four distances from a site of brief release show a rapid decrease in amplitude with distance and increase in the rise time. For a slice thickness of 400 μm there was little difference between the model that included the effects of the slice surfaces (*Eq. 2*) or simply free diffusion (*Eq. 4*) up to times of the order of 100 s. The Gaussian distribution for free diffusion (*Eq. 4*) can therefore be used to estimate the time to peak amplitude, and gives $t = r^2/6D$. From this result it is straightforward to show that the peak amplitude decreases rapidly with distance from source in proportion to $1/r^3$. These observations are shown in Fig. 6, *B–D*, where it is seen that to observe a rise time of the order of 100 s would require the source to be 220 μm distant (Fig. 6, *B* and *C*), but at that distance the amplitude is 500 times less than that at 25 μm (Fig. 6*D*). Applying this to our experimental data suggests that, although on average 3.4 μM of adenosine (or metabolites) was measured for each burst of activity, in order to have such a slow rise time the concentration at 25 μm from the site of release would be ~1.7 mM. Such a high concentration is extremely unlikely, and was never measured during our experimentation (highest concentration measured was 13 μM). The conclusion therefore is that the slow rise on the biosensor is not due to diffusion from a distal source but rather to other transport or delayed release mechanisms.

We additionally tested the model prediction that adenosine (and metabolites) will only be detected close to release sites by using multiple biosensors. We applied Mg^{2+}-free aCSF and looked for differences in responses between two biosensors (placed ~0.5 mm apart in layer V; Fig. 7*A*). In most experiments, purine currents and electrical events (fast deflections) were measured on both biosensors. However, there was con-

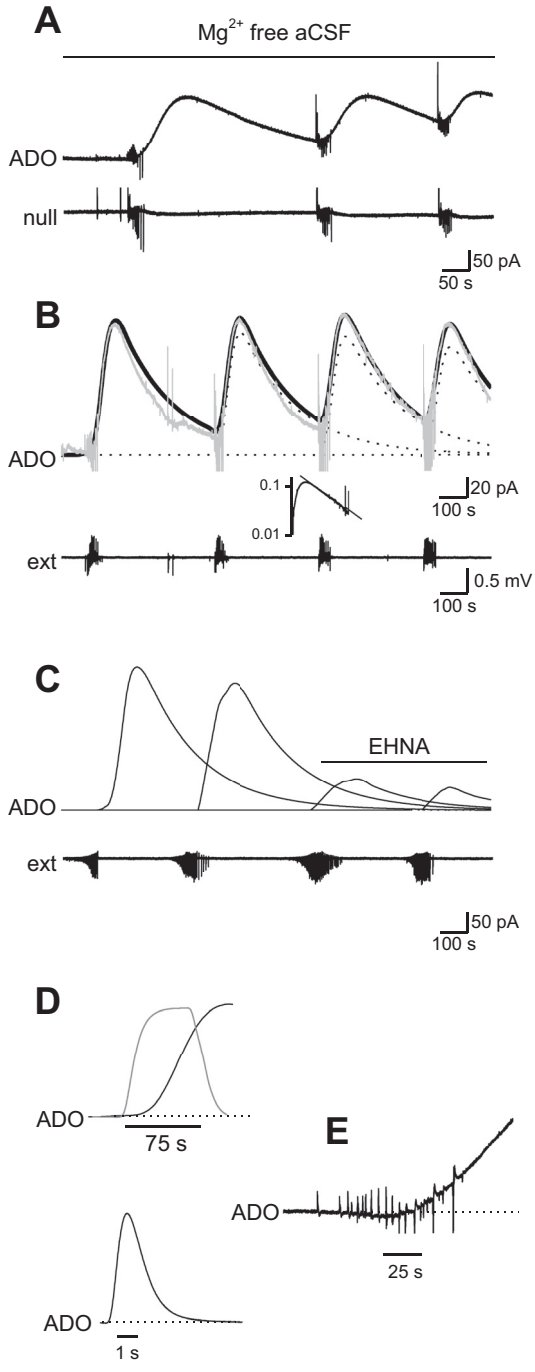

Fig. 5. Purine release during pathological network activation. *A*: ADO biosensor and null sensor during network activity. Although there are large currents following each burst on the ADO biosensor, there are no currents on the null sensor. *B*: ADO biosensor and extracellular recording during network activity; black line, model; gray line, data. Dotted line shows each separated purine waveform, with the baseline removed, allowing accurate measurement of biosensor current amplitude. *Inset*, log plot of the adenosine biosensor waveform in response to the first burst of activity. The decay is well described by a single exponential, confirming validity of deconvolution procedure. *C*: separated ADO waveforms and extracellular recording during network activity. Application of the adenosine deaminase inhibitor *erythro*-9-(2-hydroxy-3-nonyl)adenine (EHNA, 20 μM) reduced the amplitude of ADO biosensor waveforms by ~75%, confirming that the purines detected arise from either adenosine or adenosine metabolites. *D*, *top*: expanded portion of *A*, illustrating the slow rise of the ADO biosensor waveform compared with the calibration trace (bath application of 10 μM adenosine). *Bottom*: response of an ADO biosensor to the rapid application of adenosine (200-ms puff). *E*: expanded portion from *B* illustrating how the ADO biosensor waveform does not start to rise until about halfway through an ~30-s burst of network activity.

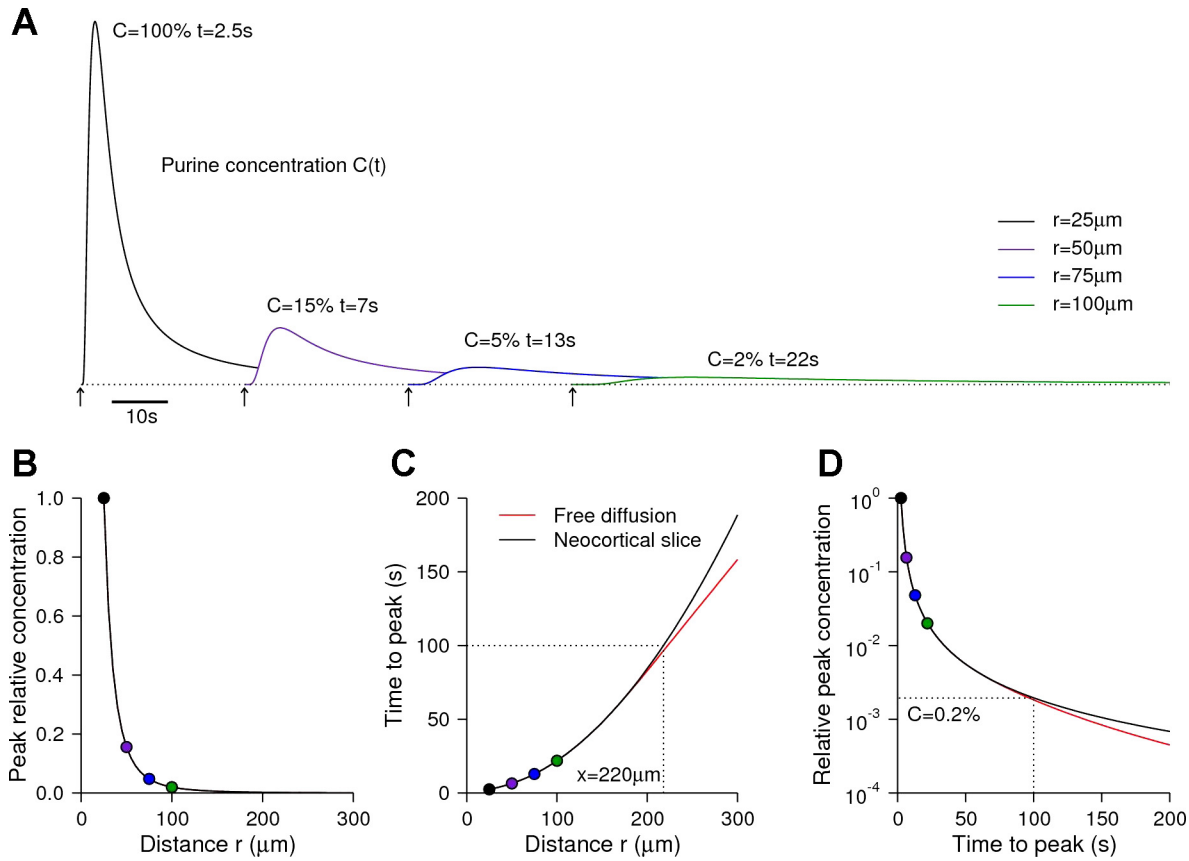

Fig. 6. Purine concentration decreases rapidly with distance because of diffusive dilution. *A*: purine waveforms (solution to *Eq. 2*) at 4 distances *r* (25, 50, 75, 100 μm) from a site of brief adenosine release. The waveform amplitude at 100 μm is 2% of that at 25 μm and has a time to peak of 22 s. *B*: the peak amplitude drops rapidly with distance, with little visible difference between the free diffusion case (*Eq. 4*) and that for neocortical slices (*Eq. 2*) for the range shown. *C*: the time-to-peak amplitude grows with the square of distance: a 100-s time to peak occurs at a distance of 220 μm. Again, little difference can be seen between the results for free diffusion (*Eq. 4*) and the slice geometry (*Eq. 2*). *D*: at a distance where the time to peak is 100 s, the relative concentration is two-thousandths that at 25 μm, suggesting that the slow time to peak is unlikely to be due to diffusion from a distant source.

siderable variation in the concentration of purine detected by each biosensor, consistent with a heterogeneous distribution of purine concentrations across the slice. In the example illustrated in Fig. 7*B*, as network activity begins, there are initially no purine currents or fast deflections, because of electrical activity present on *biosensor 1*, but clear purine currents are present on *biosensor 2*, along with deflections due to network activity. Thus the network is inactive around *biosensor 1* and the increase in purine concentration that occurs around *biosensor 2* is not detected by *biosensor 1*. Since the biosensors are ~500 μm apart, this agrees with the model predictions that virtually all of the purine released will be diluted below the level of detection once they diffuse ~300 μm. However, once network activity becomes coordinated across the slice and is detected on both biosensors, then purines are measured on both biosensors (Fig. 7*B*). However, there is no clear correlation between the amplitude of the purine waveforms present on both biosensors. These results show that adenosine and its metabolites have concentrations that are a function of the local activity and vary on a scale that is certainly < 500 μm.

Adenosine is metabolized before biosensor detection. Both experimental data and modeling suggest that the slow biosensor response time is a consequence of the release process rather than a long diffusion distance. It is possible that adenosine is metabolized before biosensor detection, since the ADO biosensor will detect adenosine and its metabolites, and this could contribute to the slow response time. To investigate this, differential measurements were made with ADO, INO, and HYP biosensors (for example, see Wall et al. 2007). If adenosine was directly detected, and there was no metabolism in the tissue, there would only be a signal on the ADO biosensor. If adenosine was metabolized to inosine, this would produce currents on ADO and INO biosensors, and if adenosine was metabolized through to hypoxanthine, this would produce currents on all three biosensors. Subtracting the calibrated biosensor signals allows for an estimation of extracellular adenosine, inosine, and hypoxanthine concentrations during activity (Wall and Dale 2007).

The three biosensors were inserted into layer V of the neocortex, and network activity was induced by zero-Mg^{2+} aCSF. During network activity, currents were measured on all three biosensors in 8 of 10 slices (Fig. 8*A*; in 2 slices there was no signal on the HYP biosensor). Addition of EHNA (20 μM), to block ADA, reduced the signal on all three biosensors (81 $\pm$ 5%, $n = 3$; Fig. 8*B*), demonstrating that the signal arises either directly from adenosine or after adenosine metabolism. The signal on the HYP biosensor directly demonstrates an increase in the extracellular concentration of hypoxanthine during activity. Thus a proportion of adenosine is metabolized to hypoxanthine by ADA and PNP. To determine whether adenosine was directly detected, currents on ADO and INO biosensors were compared. It would be predicted that the rise of the signal

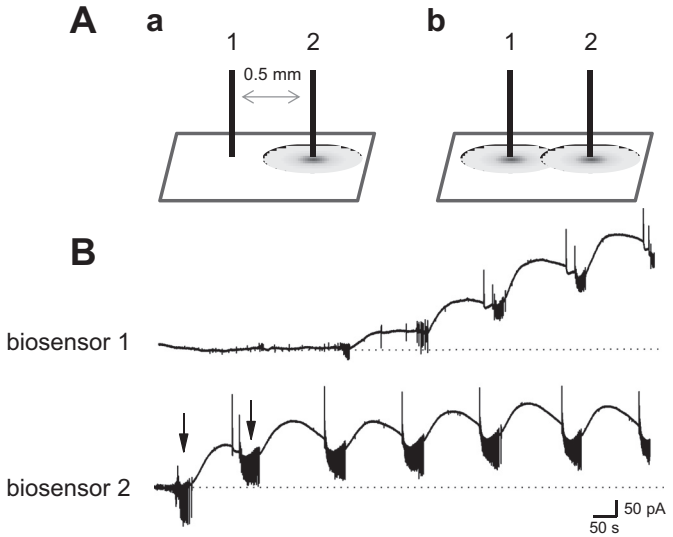

Fig. 7. Increases in purine concentration are localized. *A*: positioning of 2 biosensors (*1* and *2*) in layer V of the neocortex, with diagrams illustrating the localization of increases in extracellular purine concentration during network activity as interpreted from the biosensor traces in *B*. Network activity was induced by zero-Mg^{2+} aCSF. Initially the network [fast deflections (arrows) are electrical activity] was only active around *biosensor 1* and not around *biosensor 2*. The resultant increases in extracellular purine concentration, measured by *biosensor 1*, were not detected by *biosensor 2* (*Aa*). When the network was active around both biosensors, an increase in purine concentration was detected on both biosensors, although there was no relationship between the concentrations of purines measured (*Ab*).

on the ADO biosensor would be faster than the INO biosensor signal, as there is a metabolism step before inosine is detected. However, there was no significant difference in the rise time of the currents (Fig. 8*C*) on ADO and INO biosensors. Examination of the signals on ADO and INO biosensors within recordings from individual slices revealed no clear correlation. Sometimes large-amplitude signals occurred on the ADO biosensor with little on the INO biosensor and vice versa (for example, the INO biosensor currents are larger than ADO biosensor currents in Fig. 8*A*). This is consistent with each biosensor only detecting the purines released by local network activity, with little or no overlap on what is measured by each sensor. Thus in most slices, little adenosine is directly detected and instead most of the adenosine is metabolized before biosensor detection.

Metabolism of exogenous adenosine. To investigate adenosine metabolism in more detail, adenosine was applied to neocortical slices and the purines produced were measured with ADO, INO, and HYP biosensors inserted into layer V. Biosensor signals, scaled by calibration, were subtracted to estimate the concentrations of adenosine, inosine, and hypoxanthine in the tissue (as in Wall et al. 2007; Frenguelli et al. 2007). Constant-duration adenosine applications (50 μM, 5 min) produced 3 $\pm$ 0.2 μM adenosine in the tissue (n = 5), which represents ~6% of the applied adenosine (Fig. 9*A*). The rise time (~300–400 s) of the ADO biosensor current was significantly slower than the rise of the calibration trace (~10–15 s). Thus the ADO biosensor is only detecting the adenosine that has diffused into the slice, rather than measuring adenosine in the bath. A similar slow rise time of adenosine current was also observed with disk sensors, which have a sensing area only at the end of the biosensor that is pushed into the slice surface (n = 3). During diffusion through the slice, the adenosine produced 0.7 $\pm$ 0.2 μM inosine and 0.4 $\pm$ 0.1 μM hypoxanthine (n = 5 slices). In some slices (3 of 5) there was a clear delay (75 $\pm$ 5 s) between the initial detection of adenosine (ADO biosensor) and the detection of inosine (Fig. 9*B*). In all slices, the currents measured with INO biosensors were markedly slower to rise than currents measured on ADO biosensors (Fig. 9*B*, *inset*). The slow rise on the INO sensor was not a consequence of slower inosine diffusion in the tissue (compared to adenosine), as the rise time for bath application of inosine (50 μM) was the same for applied adenosine (see Fig. 9*A*, *inset*). When inosine was applied, a similar amount of inosine was detected in the tissue (3.0 $\pm$ 0.8 μM) compared with adenosine application, although more hypoxanthine was detected (2.0 $\pm$ 0.1 μM). Interestingly, there was no clear delay between the currents on the INO and HYP biosensors (Fig. 9*C*). This is consistent with most of the adenosine being removed before it reaches the biosensor and the slow production of metabolites.

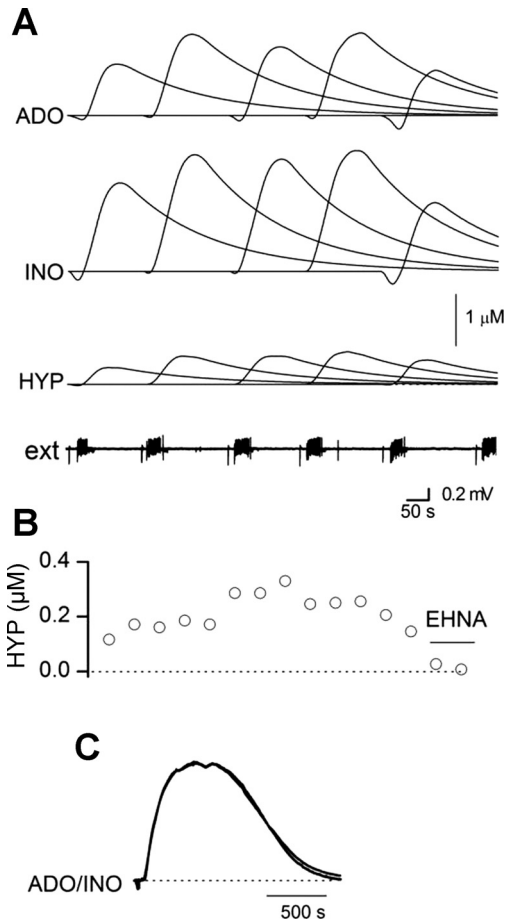

Fig. 8. The major purines detected are adenosine metabolites. *A*: separated waveforms from ADO, INO, and HYP biosensors with trace from extracellular recording electrode during pathological network activity, induced by zero-Mg^{2+} aCSF. Traces have been corrected for biosensor sensitivity (measured from calibration). *B*: graph plotting the concentration of hypoxanthine against burst number. EHNA blocked hypoxanthine detection; thus the hypoxanthine arises from adenosine metabolism. *C*: superimposed traces from ADO and INO biosensors following a single burst of activity. After normalization, the waveforms had virtually identical kinetics. This strongly suggests that adenosine metabolites are detected rather than adenosine itself.

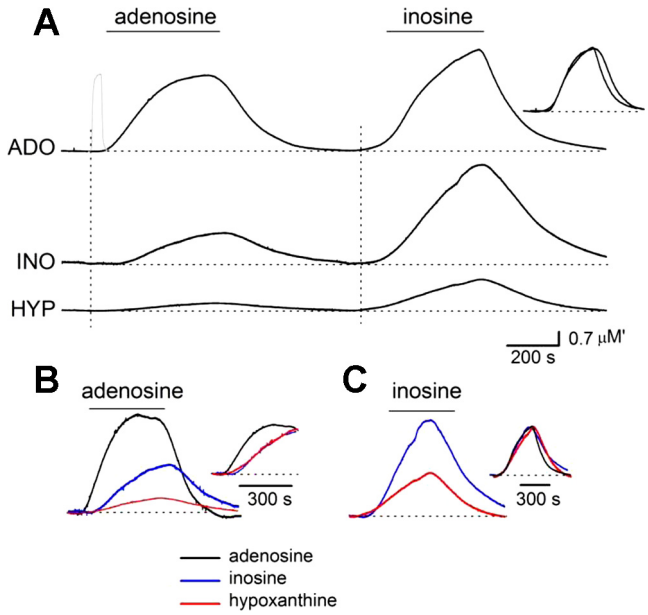

Fig. 9. Neocortical adenosine metabolism. *A*: traces from ADO, INO, and HYP biosensors after bath application of 50 μM adenosine and then 50 μM inosine. The currents have been corrected for biosensor sensitivity (from the calibration). The gray line is the calibration trace for the ADO biosensor (10 μM adenosine, no tissue present), illustrating the slow rise and decay of the signals measured in tissue. *Inset*, responses from the ADO biosensor to application of adenosine and to inosine normalized and superimposed to show a similar speed of response. *B*: traces from *A* corrected for biosensor sensitivity and then subtracted to give the adenosine, inosine, and hypoxanthine concentration profiles after bath application of adenosine. *Inset*, traces from *B* normalized to illustrate differences in the time course of adenosine, inosine, and hypoxanthine waveforms. *C*: traces from *A* corrected for biosensor sensitivity and then subtracted to give the inosine and hypoxanthine concentration profiles after bath application of inosine. *Inset*, traces from *C* normalized and aligned to illustrate the time courses of inosine and hypoxanthine detection. The black line is the inosine response from the ADO biosensor, illustrating that the ADO biosensor has a comparable response time to the INO and HYP biosensors.

DISCUSSION

We have investigated the properties of adenosine signaling in the neocortex using in vitro models of low-rate activity (excitant solution) and high-rate pathological activity (zero-Mg^{2+} aCSF). Both of these patterns of network activity were strongly attenuated by activation of adenosine A_1 receptors and were enhanced by blocking A_1 receptors with an antagonist. Although this has been previously reported for high-rate activity (O'Shaughnessy et al. 1988), this is the first report of a role for adenosine in controlling low-rate activity and shows that neocortical A_1 receptors were neither fully occupied (saturated) or unoccupied during either low- or high-rate activity. As the extracellular concentration of adenosine sits toward the middle of the concentration response for A_1 receptors, small changes in adenosine concentration will have large effects on network activity. Thus neocortical adenosinergic signaling is a negative-feedback mechanism with a wide dynamic range and is able to control network activities that vary from low-frequency single events to prolonged high-frequency bursts.

Localized increases in extracellular adenosine concentration. During pathological, high-rate activity sufficient adenosine was released into the extracellular space to be detected with a biosensor, as also observed for hippocampal seizures (Dale and Frenguelli 2009; Etherington et al. 2009). Experimental data from multiple biosensors supported by computational modeling show that the increase in extracellular adenosine and metabolite concentration was not homogeneous across the neocortex but was instead highly localized. Adenosine did not flood as a wave across tissue, but instead the concentration of adenosine was determined by local network activity, with increases in extracellular adenosine concentration becoming uncorrelated over very short distances, which are certainly $<$ 500 μm.

During low-rate activity (single and groups of population spikes), adenosine (and metabolites) could not be directly measured with a biosensor. However, when A_1 receptors were blocked, there was an increase in the probability of a network event occurring within a short interval after the previous event, which is consistent with the pulsatile release of adenosine. Since the K_d for A_1 receptors is low (between 70 and 300 nM; Dunwiddie and Masino 2001; Fredholm et al. 2001) and the concentration of adenosine falls very rapidly during diffusion, if adenosine release is very proximal to the receptors, it is feasible for the localized release of adenosine to modulate activity but not be detected by a biosensor. The minimal detectable increase in the extracellular concentration of adenosine (or metabolite) is ~25 nM (assuming a sensitivity of the ADO biosensor of at least ~2,000 pA for 10 μM adenosine, which would give currents on the order of ~2–5 pA). In the hippocampus, an increase in extracellular adenosine (or metabolite) concentration could be detected with a biosensor after a single population spike (Wall and Dale 2013). However, the currents measured were small (~2 pA) and only observed in a minority of slices. Similar release may occur in the neocortex, but if the number of activated fibers/cells is smaller than in the hippocampus and there is a longer diffusion distance between the release sites and the biosensor, then the concentration of adenosine released will fall below the limits of biosensor detection.

Instead of pulsatile adenosine release, there could be a basal homogeneous extracellular tone of adenosine, which acts to dampen down network excitability. Because modeling and experimental data suggest that adenosine is rapidly diluted during diffusion, a homogeneous global extracellular tone would require the coordinated release of adenosine from multiple release sites across the tissue. It is much more likely that the extracellular concentration of adenosine will vary depending on local network activity. This is in keeping with previous experimental evidence for such local variation seen by the effects of blocking A_1 receptors on synaptic transmission between pairs of layer V pyramidal cells: There was marked variation in the degree of A_1 receptor activation between synapses in slices from the same animal and even between reciprocal synapses within the same slice (Kerr et al. 2013). Thus adenosine signaling provides a targeted negative-feedback mechanism for the fine, local control of network activity.

With pathological high-rate activity inosine, not adenosine, is detected by biosensors. Evidence from differential biosensor measurements suggests that the major purines detected during high-rate pathological activity were the adenosine metabolites inosine and hypoxanthine rather than adenosine itself. Blocking ADA markedly reduced the amplitude of currents on all biosensors, and thus the inosine and hypoxanthine arise from adenosine metabolism (Klyuch et al. 2011; Wall and Dale 2007). There was no clear difference in the rise of currents measured on ADO and INO biosensors. If adenosine was

directly detected, then the signal on the INO biosensor would be expected to be slower or delayed compared with the signal on the ADO biosensor, as metabolism of adenosine would have to occur before inosine detection. This was confirmed in experiments in which adenosine was exogenously applied to slices and the signal on the INO biosensor was much slower than the ADO biosensor signal. A similar delay in inosine production has also been observed in the cerebellum and in the hippocampus (Frenguelli et al. 2007; Wall et al. 2007). Once produced, inosine is metabolized to hypoxanthine by PNP, which, like ADA, is mainly an intracellular enzyme (Bzowska et al. 2000). Therefore adenosine is transported into cells, metabolized, and then effluxed back into the extracellular space before detection. The slow rise of the currents on all biosensors (on the order of 100 s) is consistent with these intervening metabolic and uptake/efflux steps.

Modes of adenosine removal. Our data are consistent with a small amount of adenosine being released during low-rate network activity, which is rapidly diluted and actively removed before biosensor detection. Although the model included no active removal processes, just diffusion, it showed that the concentration of adenosine rapidly falls because of diffusion, providing an upper range on the distance of adenosine transport. Addition of active removal mechanisms would produce an even more rapid fall in concentration. Previous studies suggest that the major method of active adenosine removal, under basal conditions, is uptake into cells, by equilibrative nucleoside transporters (ENTs), and subsequent conversion to AMP by ADK (Dunwiddie and Masino 2001). Thus blocking either ADK or ENTs increases the extracellular concentration of adenosine and inhibits synaptic transmission via A_1 receptor activation (Atterbury and Wall 2009; Etherington et al. 2009; Wall et al. 2007). In contrast, metabolism to inosine by ADA plays only a minor role in adenosine removal when there is little network activity. Thus blocking ADA activity has little effect on the extracellular concentration of adenosine and synaptic transmission (Atterbury and Wall 2009; Pak et al. 1994; Wall et al. 2007; Zhu and Krnjevic 1994). If however, ADK is blocked, then inhibition of ADA has a much larger effect on adenosine removal (for example, see Atterbury and Wall 2009). Thus it is predicted that with small amounts of adenosine released the fall in concentration is dominated by diffusion with subsequent conversion of adenosine to AMP by ADK.

Our data from pathological high-rate network activity are consistent with a more significant role for ADA in adenosine removal (Latini and Pedata 2001; Lloyd and Fredholm 1995). With high-rate activity, the large amount of adenosine released saturates ADK (K_m ~2 μm; Phillips and Newsholme 1979) and some adenosine escapes conversion to AMP and is instead deaminated by ADA (K_m ~47 μm; Geiger and Nagy 1986) to produce inosine. Since the concentration of extracellular adenosine falls rapidly, the high concentration of inosine inside the cell leads to efflux, down the concentration gradient, and detection by the biosensor. This is consistent with previous studies in the hippocampus where, for example, blocking ADK increased the basal concentrations of adenosine but had little effect on the purine efflux produced by seizures since it is saturated (Etherington et al. 2009). Thus even during high-rate neocortical activity adenosine is not directly measured. The extracellular concentration falls rapidly because of diffusion and uptake, and only an indirect measurement of adenosine is possible when one of the removal mechanisms becomes saturated. The efficiency of adenosine removal/inactivation ensures the localization of signaling and thus allows fine control over small regions of the network.

GRANTS

This work was funded by Biotechnology and Biological Sciences Research Council (BBSRC) Grant No. BB/J015369/1.

DISCLOSURES

No conflicts of interest, financial or otherwise, are declared by the author(s).

AUTHOR CONTRIBUTIONS

Author contributions: M.J.W. and M.J.E.R. conception and design of research; M.J.W. performed experiments; M.J.E.R. performed modeling; M.J.W. and M.J.E.R. analyzed data; M.J.W. and M.J.E.R. interpreted results of experiments; M.J.W. and M.J.E.R. prepared figures; M.J.W. drafted manuscript; M.J.W. and M.J.E.R. edited and revised manuscript; M.J.W. and M.J.E.R. approved final version of manuscript.

REFERENCES

Agarwal RP, Spector T, Parks RE. Tight-binding inhibitors. IV. Inhibition of adenosine deaminase by various inhibitors. *Biochem Pharmacol* 26: 359–367, 1997.

Atterbury A, Wall MJ. Adenosine signalling at immature parallel fibre-Purkinje cell synapses in rat cerebellum. *J Physiol* 587: 4497–4508, 2009.

Boison D. Adenosine as a neuromodulator in neurological diseases. *Curr Opin Pharmacol* 8: 2–7, 2008.

Boison D. Adenosine-based modulation of brain activity. *Curr Neuropharmacol* 7: 158–159, 2009.

Bzowska A, Kulikowska E, Shugar D. Purine nucleoside phosphorylase: properties, functions and clinical aspects. *Pharmacol Ther* 88: 349–425, 2000.

Dale N, Frenguelli BG. Release of adenosine and ATP during ischemia and epilepsy. *Curr Neuropharmacol* 7: 160–179, 2009.

Dale N, Pearson T, Frenguelli BG. Direct measurement of adenosine release during hypoxia in the CA1 region of the rat hippocampal slice. *J Physiol* 526: 143–155, 2000.

Dunwiddie TV, Masino S. The role and regulation of adenosine in the central nervous system. *Annu Rev Neurosci* 24: 31–55, 2001.

During MJ, Spencer DD. Adenosine: a potential mediator of seizure arrest and postictal refractoriness. *Ann Neurol* 32: 618–624, 1992.

Etherington LA, Patterson GE, Meechan L, Boison D, Irving AJ, Dale N, Frenguelli BG. Astrocytic adenosine kinase regulates basal synaptic adenosine levels and seizure activity but not activity-dependent adenosine release in the hippocampus. *Neuropharmacology* 56: 429–437, 2009.

Fredholm BB. Adenosine and neuroprotection. *Int Rev Neurobiol* 40: 259–280, 1996.

Fredholm BB, Arslan G, Halldner L, Kull B, Schulte G, Wasserman W. Structure and function of adenosine receptors and their genes. *Naunyn Schmiedebergs Arch Pharmacol* 362: 364–374, 2000.

Fredholm BB, Irenius E, Kull B, Schulte G. Comparison of the potency of adenosine as an agonist at human adenosine receptors in Chinese hamster ovary cells. *Biochem Pharmacol* 61: 443–448, 2001.

Frenguelli BG, Wigmore G, Llaudet E, Dale N. Temporal and mechanistic dissociation of ATP and adenosine release during ischaemia in the mammalian hippocampus. *J Neurochem* 101: 1400–1413, 2007.

Frohlich F, McCormick DA. Endogenous electric fields may guide neocortical network activity. *Neuron* 67: 129–143, 2010.

Geiger JD, Nagy JI. Distribution of adenosine deaminase activity in rat brain and spinal cord. *J Neurosci* 6: 2707–2714, 1986.

Grenier F, Timofeev I, Steriade M. Neocortical very fast oscillations (ripples, 80–200 Hz) during seizures: intracellular correlates. *J Neurophysiol* 89: 841–852, 2003.

Gulyás-Kovács A, Dóczi J, Tarnawa I, Détári L, Banczerowski-Pelyhe I, Világi I. Comparison of spontaneous and evoked epileptiform activity in three in vitro epilepsy models. *Brain Res* 945: 174–180, 2002.

Kerr M, Wall MJ, Richardson MJ. Adenosine A_1 receptor activation mediates the developmental shift at layer 5 pyramidal cell synapses and is a determinant of mature synaptic strength. *J Physiol* 591: 3371–3380, 2013.

Kimura M, Saitoh N, Takahashi T. Adenosine A1 receptor-mediated presynaptic inhibition at the calyx of Held of immature rats. *J Physiol* 553: 415–426, 2003.

Klyuch BP, Richardson MJ, Dale N, Wall MJ. The dynamics of single spike-evoked adenosine release in the cerebellum. *J Physiol* 589: 283–295, 2011.

Latini S, Pedata F. Adenosine in the central nervous system: release mechanisms and extracellular concentrations. *J Neurochem* 79: 463–484, 2001.

Llaudet E, Botting NP, Crayston JA, Dale N. A three-enzyme microelectrode sensor for detecting purine release from central nervous system. *Biosens Bioelectron* 18: 43–52, 2003.

Lloyd HG, Fredholm BB. Involvement of adenosine deaminase and adenosine kinase in regulating extracellular adenosine concentration in rat hippocampal slices. *Neurochem Int* 26: 387–395, 1995.

Lovatt D, Xu Q, Liu W, Takano T, Smith NA, Schnermann J, Tieu K, Nedergaard M. Neuronal adenosine release, and not astrocytic ATP release, mediates feedback inhibition of excitatory activity. *Proc Natl Acad Sci USA* 109: 6265–6270, 2012.

Mitchell JB, Lupica CR, Dunwiddie TV. Activity-dependent release of endogenous adenosine modulates synaptic responses in rat hippocampus. *J Neurosci* 13: 3439–3447, 1993.

Mody I, Lambert JD, Heinemann U. Low extracellular magnesium induces epileptiform activity and spreading depression in rat hippocampal slices. *J Neurophysiol* 57: 869–888, 1987.

Ochiishi T, Chen L, Yukawa A, Saitoh Y, Sekino Y, Arai T, Nakata H, Miyamoto H. Cellular localization of adenosine A1 receptors in rat forebrain: immunohistochemical analysis using adenosine A1 receptor-specific monoclonal antibody. *J Comp Neurol* 411: 301–316, 1999.

Oliet SH, Poulain DA. Adenosine-induced presynaptic inhibition of IPSCs and EPSCs in rat hypothalamic supraoptic nucleus neurones. *J Physiol* 520: 815–825, 1999.

O'Shaughnessy CT, Aram JA, Lodge D. A1 adenosine receptor-mediated block of epileptiform activity induced in zero magnesium in rat neocortex in vitro. *Epilepsy Res* 2: 294–301, 1988.

Pajski ML, Venton BJ. Adenosine release evoked by short electrical stimulations in striatal brain slices is primarily activity dependent. *ACS Chem Neurosci* 12: 775–787, 2010.

Pak MA, Hass HL, Decking UK, Schrader J. Inhibition of adenosine kinase increases endogenous adenosine and depresses neuronal activity in hippocampal slices. *Neuropharmacology* 33: 1049–1053, 1994.

Parga N, Abbott LF. Network model of spontaneous activity exhibiting synchronous transitions between up and down states. *Front Neurosci* 1: 57, 2007.

Pearson T, Nuritova F, Caldwell D, Dale N, Frenguelli BG. A depletable pool of adenosine in area CA1 of the rat hippocampus. *J Neurosci* 21: 2298–2307, 2001.

Phillips E, Newsholme EA. Maximum activities, properties and distribution of 5′ nucleotidase, adenosine kinase and adenosine deaminase in rat and human brain. *J Neurochem* 33: 553–558, 1979.

Richardson MJ, Silberberg G. Measurement and analysis of postsynaptic potentials using a novel voltage-deconvolution method. *J Neurophysiol* 99: 1020–1031, 2008.

Rivkees SA, Price SL, Zhou FC. Immunohistochemical detection of A_1 adenosine receptors in rat brain with emphasis on localization in the hippocampal formation, cerebral cortex, cerebellum and basal ganglia. *Brain Res* 677: 193–203, 1995.

Sanchez-Vives MV, McCormick DA. Cellular and network mechanisms of rhythmic recurrent activity in neocortex. *Nat Neurosci* 3: 1027–1034, 2000.

Silberberg G, Wu C, Markram H. Synaptic dynamics control the timing of neuronal excitation in the activated neocortical microcircuit. *J Physiol* 556: 19–27, 2004.

Steriade M, Nunez A, Amzica F. A novel slow (<1 Hz) oscillation of neocortical neurons in vivo: depolarizing and hyperpolarizing components. *J Neurosci* 13: 3252–3265, 1993.

Traub RD, Jefferys JG, Whittington MA. Enhanced NMDA conductance can account for epileptiform activity induced by low Mg^{2+} in the rat hippocampal slice. *J Physiol* 478: 379–393, 1994.

van Aerde KI, Qi G, Feldmeyer D. Cell type-specific effects of adenosine on cortical neurons. *Cereb Cortex* (October, 9, 2013). doi:10.1093/cercor/bht274.

Wall MJ, Atterbury A, Dale N. Control of basal extracellular adenosine concentration in rat cerebellum. *J Physiol* 582: 137–153, 2007.

Wall MJ, Dale N. Auto-inhibition of rat parallel fibre-Purkinje cell synapses by activity-dependent adenosine release. *J Physiol* 581: 553–565, 2007.

Wall MJ, Dale N. Activity-dependent release of adenosine: a critical re-evaluation of mechanism. *Curr Neuropharmacol* 6: 329–337, 2008.

Wall MJ, Dale N. Neuronal transporter and astrocytic ATP exocytosis underlie activity-dependent adenosine release in the hippocampus. *J Physiol* 591: 3853–3871, 2013.

Wall MJ, Eason R, Dale N. Biosensor measurement of purine release from cerebellar cultures and slices. *Purinergic Signal* 6: 339–348, 2010.

Wong YC, Billups B, Johnston J, Evans RJ, Forsythe ID. Endogenous activation of adenosine A1 receptors but not P2X receptors during high-frequency synaptic transmission at the calyx of Held. *J Neurophysiol* 95: 3336–3342, 2006.

Zhu PJ, Krnjevic K. Endogenous adenosine deaminase does not modulate synaptic transmission in rat hippocampal slices under normoxic or hypoxic conditions. *Neuroscience* 63: 489–497, 1994.